

# Method and Model for a Highly Realistic Rendering of a Three-Dimensional Image

Mykola Nechyporuk, Olexander Romanyuk

**Abstract**— The formation of color components of face images is a complex computational task, since for each pixel of a surface it is necessary to calculate the color intensity, for which it is necessary to determine the unit vectors to the light source and normal to the surface. Therefore, the urgent task is to simplify the coloring procedure without losing the realism of the final image. It is suggested to use second-degree and third-degree polynomials to adapt to painting, depending on the surface curvature. For the third degree polynomial, an approximation formula is obtained to determine the diffuse and specular color components. The hardware for determining the coefficients and the approximation polynomial is proposed.

**Keywords**—rendering, diffuse and specular color components, 3D imaging, plastic surgery, face image.

## I. INTRODUCTION

Spatial imaging [5, 7, 13, 14, 15-18] is a complex computational process. This is due to the multistepness and complexity of geometric transformations, the use of complex models of lighting and over-painting. The final rendering (rendering) stage [1, 7] is one of the most time consuming, as each intensity point determines the color intensity and the screen coordinates. It is important not only to accurately reproduce the shape of the object and its design features, but also to correctly convey the gradation of colors, since this is crucial in creating the illusion of three-dimensional volume on a two-dimensional flat screen.

In determining the intensity of the color of the pixels, the location of the light source and the observer, the optical properties of the material, the spectral characteristics of the light source, and the curvature of the surface are taken into account. In this regard, the final visualization is characterized by significant computational costs, which necessitates the development of methods and tools to improve the productivity of its implementation.

At the present stage of development of three-dimensional graphics the question of dynamic graphic images formation in real time and in interactive mode is urgently raised, when it is assumed that the trajectories of motion of objects are not predetermined but determined by the actions of the user in the process of interaction with the system. Visualization of three-dimensional scenes for such modes imposes strict requirements on methods and means of forming three-dimensional graphic scenes, which creates the task of increasing their productivity.

Today, the growth rate of geometric complexity of 3D images exceeds the growth rate of graphics performance [7]. Insufficient graphics performance is also a hindrance to modeling in physical process scenes and increasing the number of dynamic objects.

Since the final visualization stage is the most time-consuming stage of 3D modeling and accounts for 60-80% [15] of the total amount of calculations, it is advisable to develop methods and models that would improve the performance and achieve the desired dynamics of realistic images.

The purpose and objectives of the study. The purpose of the work is to increase the productivity of 3D image formation by using new models and the painting method.

The object of study – the process of finally rendering three-dimensional graphic objects in

computer graphics systems.

Subject of study – methods and tools for improving productivity of final visualization of three-dimensional objects.

Research methods. In the course of the study applied: theory of numbers and numerical methods; theory of algorithms; theory of interpolation of functions; methods of analytical geometry, linear algebra, differential and integral calculus; computer simulation to analyze and verify the validity of theoretical findings

Scientific novelty of the results.

1. The method of painting is developed, the peculiarity of which is the adaptive use for determining the intensities of color in different parts of the surface of the polynomials of the second and third degrees, which allowed to increase the productivity of forming a three-dimensional image, and, as a consequence, to provide a dynamic mode of display.

2. New modifications of the Cook-Torrence and Vard models are proposed, which differ from the known ones when calculating only one function and smaller degrees of polynomials, which makes it possible to improve the performance of three-dimensional image formation taking into account the offset properties of surfaces.

The practical significance of the obtained results is that, on the basis of theoretical studies and scientific results obtained, software and hardware for the formation of three-dimensional images have been developed.

Publications. Subjects of the research are published: scientific work, of which 1 monograph; articles included in Scopus international scientific base; articles in publications included in the list of professional publications; certificates for registration of copyright on computer programs.

## II. ANALYTICAL REVIEW OF LITERATURE

Diffuse reflection is characteristic of matte and rough surfaces with chaotic irregularities whose dimensions are comparable to or exceeds the wavelength. Diffuse reflection determines the visibility of surrounding bodies because each point of the illuminated surface emits reflected rays in all directions. In the presence of a point light source in the scene, the intensity of the diffuse reflection is proportional to the cosine of the angle between the normal to the surface and the direction to the light source [3, 7, 13, 14]. In this case, the Lambert cosine law is used to calculate the diffuse reflection intensity [7]

$$I_d = I_0 \cdot k_d \cdot \cos \varphi,$$

where  $I_0$  - the intensity of the light source,  $k_d \in [0, 1]$  - diffuse reflection coefficient,  $\varphi$  - the angle between the vector  $\vec{L}$  and the normal  $\vec{N}$  to the surface (Fig. 1).

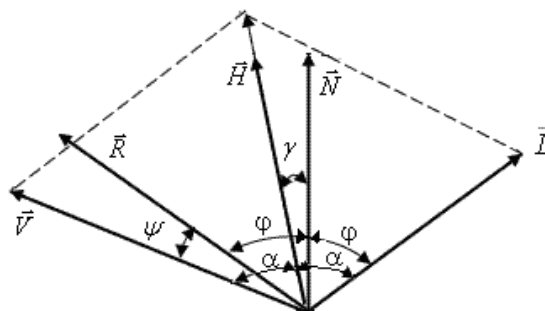


Fig. 1 The normal vector to the surface point

Computer graphics most often use the model of determining the speculative component of Phong color [3, 7, 13, 14], which has the form

$$I_s = I \cdot \varpi(\varphi, \lambda) \cdot \cos^n \psi,$$

where  $\varpi(\varphi, \lambda)$  - reflectance curve, which determines the ratio of mirror reflected light to the incident as a function of the angle of incidence  $\theta$  and wavelength  $\lambda$ ,  $n$  - surface speculation coefficient.

Function  $\varpi(\varphi, \lambda)$  is complex complex, so in most cases it is replaced by a constant  $k_s$  which is determined experimentally or chosen for aesthetic reasons. In Phong BRDF [1, 3, 7]  $\cos \psi = \vec{V} \cdot \vec{R}$  where  $\vec{R} = 2 \cdot (\vec{L} \cdot \vec{N}) \cdot \vec{N} - \vec{L}$ . Vector  $\vec{R}$  called specular reflection. [7] In the distributive function of Blin which historically was later Phong BRDF instead  $\cos \psi$  use  $\cos \gamma = \vec{N} \cdot \vec{H}$  where  $\vec{H} = (\vec{L} + \vec{V}) / |\vec{L} + \vec{V}|$ .

In most cases, when painting by Phong, models of Blin and Phong lighting are used [3, 7, 13, 14]. This is due to the fact that the specified BRDF are derived from the cosine of the angle between vectors that are easily found through their scalar product. When the light source and the observer are at a sufficient distance from the object (the most common case in a computer graphic), the vector  $\vec{H}$  of Blin model calculated once for each triangle. In connection with this, in most cases for painting surfaces by Phong method is used lighting model of Blin.

Determining diffuse and specular color components is a complex computational task [2], which involves the development of new methods and tools.

### III. MODIFICATION OF EXISTING METHODS OF VISUALIZATION OF OFFSET FACE SKIN STRUCTURE

Testing [4, 9, 10, 11] with subsequent illumination is most often used in the formation of images of a person's face for surgical interventions. In this case, the surface area of the image obtained from patients' photographs is used as texture. This approach best conveys the relief character of the skin, its specific micro-features [7,13].

The surfaces of virtually all materials have the property of anisotropy, that is, the reflectivity of the material depends on the angle of view of the object by the observer relative to the normal to the surface.

As the skin belongs to rough surfaces, it is often advisable to use lighting models that take into account the offset structure of the surface and, as a consequence, are more physically correct. Such models include the Cook-Torrence model and the Vard model [7,13,14].

It was found [2] that the Cook-Torrence model better models the spectral component of color, and the Vard model diffuses.

In these models, the surface roughness distribution is used to account for surface roughness.

Consider the Cook-Torrence model [7, 14], the bend with which the calculation of reflected light is carried out by the formula

$$\frac{F \cdot G \cdot D}{(\vec{V} \cdot \vec{N}) \cdot (\vec{L} \cdot \vec{N})},$$

where  $F$  - coefficient of Frenel  $G$  - an option that allows self-shading fields,  $D$  - a parameter that determines the rms slope of the microgranules.

Microgranules have the greatest impact if they are directed along the vector  $\vec{H}$ . Parameter  $D$  determined by the following formula

$$D = \frac{1}{4 \cdot m^2 (\vec{H} \cdot \vec{N})^4} e^{\left( \frac{(\vec{H} \cdot \vec{N})^2 - 1}{m^2 \cdot (\vec{H} \cdot \vec{N})^2} \right)}$$

where  $m$  - an average slope of the microgranules.  $m$  is selected in the range from 0.2 to 0.6.

Calculation  $D$  is difficult as it involves the use of two functions - exponential and cosine. We will express  $D$  through one function that will simplify the computational process.

Write parameter that determines the degree exponent in the formula for calculating  $D$  in this form

$$\frac{(\vec{H} \cdot \vec{N})^2 - 1}{m^2 \cdot (\vec{H} \cdot \vec{N})^2} = \frac{\cos^2 - 1}{m^2 \cdot \cos^2} = \frac{-\sin^2(\gamma)}{m^2 \cdot \cos^2(\gamma)} = -\frac{\text{tg}^2(\gamma)}{m^2}$$

With this in mind, the following formula can be written to determine  $D$

$$D = \frac{e^{-\frac{\text{tg}^2(\gamma)}{m^2}}}{4 \cdot m^2 (\vec{H} \cdot \vec{N})^4}$$

Decompose  $e^{-\frac{\text{tg}^2(\gamma)}{m^2}}$  in Taylor, limited to two terms

$$e^{-\frac{\text{tg}^2(\gamma)}{m^2}} \approx 1 - \frac{x^2}{m^2}$$

Approximate  $e^{-\frac{\text{tg}^2(\gamma)}{m^2}}$  by function  $\cos \frac{a}{m^2}$

Decompose  $\cos \frac{a}{m^2}$  in Taylor, limited to two terms.

$$\cos \frac{a}{m^2} = 1 - \frac{a}{2 \cdot m^2} \cdot x^2$$

Equating the right parts of the two schedules to the Taylor series, we obtain this equality

$$1 - \frac{x^2}{m^2} = 1 - \frac{a}{2 \cdot m^2} \cdot x^2$$

From the last equation we find that  $a = 2$

As follows,

$$e^{-\frac{\text{tg}^2(\gamma)}{m^2}} \approx \cos \frac{2}{m^2}(\gamma)$$

Considering

$$D = \frac{1}{4 \cdot m^2 (\vec{H} \cdot \vec{N})^4} e^{\left(\frac{(\vec{H} \cdot \vec{N})^2 - 1}{m^2 \cdot (\vec{H} \cdot \vec{N})^2}\right)} = \frac{1}{4 \cdot m^2 (\vec{H} \cdot \vec{N})^4} \cos^{\frac{2}{m^2}}(\gamma).$$

Given that the scalar product of vectors  $\vec{H}$  and  $\vec{N}$  is  $\cos \gamma$ , we write the following expression for  $D$

$$D = \frac{1}{4 \cdot m^2 \cdot (\vec{H} \cdot \vec{N})^4} \cos^{\frac{2}{m^2}}(\gamma) = \frac{1}{4 \cdot m^2 \cdot \cos^4(\gamma)} \cos^{\frac{2}{m^2}}(\gamma) = \frac{\cos^{\frac{2}{m^2}-4}(\gamma)}{4 \cdot m^2}.$$

Fig. 2 shows a graphic  $\frac{\cos^{\frac{2}{m^2}-4}(\gamma)}{4 \cdot m^2}$  and  $\frac{e^{\frac{\text{tg}^2(\gamma)}{m^2}}}{4 \cdot m^2 \cos^4 \gamma}$ .

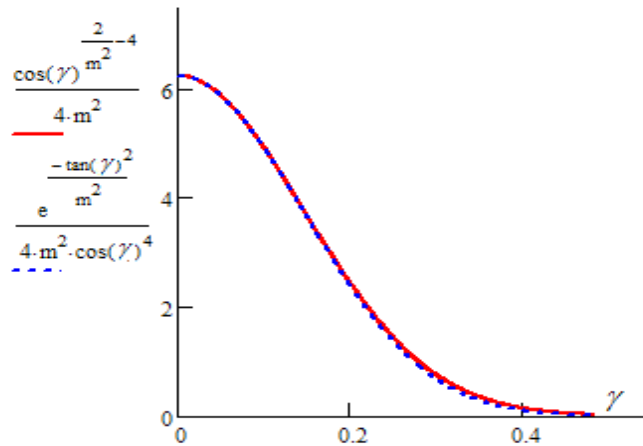


Fig. 2 Graphic of functions  $\frac{\cos^{\frac{2}{m^2}-4}(\gamma)}{4 \cdot m^2}$  and  $\frac{e^{\frac{\text{tg}^2(\gamma)}{m^2}}}{4 \cdot m^2 \cos^4 \gamma}$ .

The graph shows that the proposed function has a good convergence of the original.

$$\frac{e^{\frac{\text{tg}^2(\gamma)}{m^2}}}{4 \cdot m^2 \cos^4 \gamma}$$

Fig. 3 shows a graph of the relative approximation error function  $\frac{\cos^{\frac{2}{m^2}-4}(\gamma)}{4 \cdot m^2}$  the angle  $\gamma$ .

$$\frac{\cos^{\frac{2}{m^2}-4}(\gamma)}{4 \cdot m^2}$$

the angle  $\gamma$ .

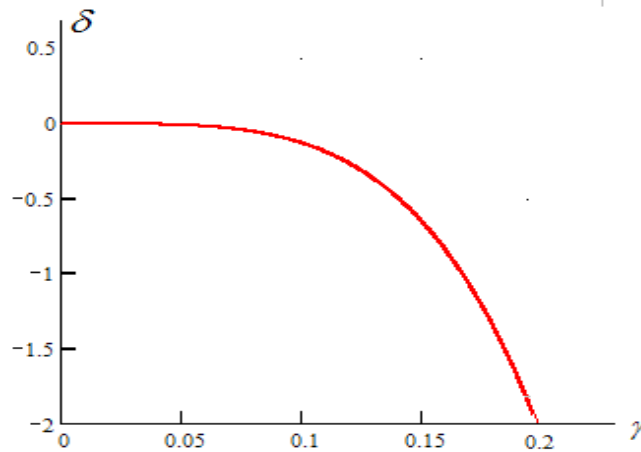


Fig. 3 - The graph of change of relative error of approximation of function  $\frac{e^{-\frac{tg^2(\gamma)}{m^2}}}{4 \cdot m^2 \cos^4 \gamma}$  by

$$\text{function } \frac{\cos^{\frac{2}{m^2}-4}(\gamma)}{4 \cdot m^2} \text{ from the angle } \gamma$$

The graph above shows that high approximation accuracy is achieved for a significant change interval of the original function.

We got function  $\cos^n \gamma \approx \left( \frac{n}{g} (\cos \gamma - 1) + 1 \right)^g$ .

Use this function to approximate D:

$$\frac{\cos^{\frac{2}{m^2}-4}(\gamma)}{4 \cdot m^2} \approx \frac{1}{4 \cdot m^2} \cdot \left( \frac{\frac{2}{m^2}-4}{g} \cdot (\cos \gamma - 1) + 1 \right)^g.$$

After simplification we get that  $\frac{\cos^{\frac{2}{m^2}-4}(\gamma)}{4 \cdot m^2} = \frac{1}{4 \cdot m^2} \left( \frac{2}{m^2} - 4 \cdot (\cos \gamma - 1) + 1 \right)^g$

For  $g = 4$   $D4 = \frac{1}{4 \cdot m^2} \cdot \left[ \left( \frac{1}{2m^2} - 1 \right) \cdot (\cos \gamma - 1) + 1 \right]^4$ ,

For  $g = 8$   $D8 = \frac{1}{4 \cdot m^2} \cdot \left[ \left( \frac{1}{4 \cdot m^2} - \frac{1}{2} \right) \cdot (\cos(\gamma) - 1) + 1 \right]^8$ ,

For  $g = 16$   $D16 = \frac{1}{4 \cdot m^2} \cdot \left[ \left( \frac{1}{8 \cdot m^2} - \frac{1}{4} \right) \cdot (\cos(\gamma) - 1) + 1 \right]^{16}$ .

Fig. 4 shows a graph of changing D, D4, D8, D16. Function D16 provided high accuracy of approximation as for the epicenter of the bell-shaped D, and for its blooming zone (Fig. 5).

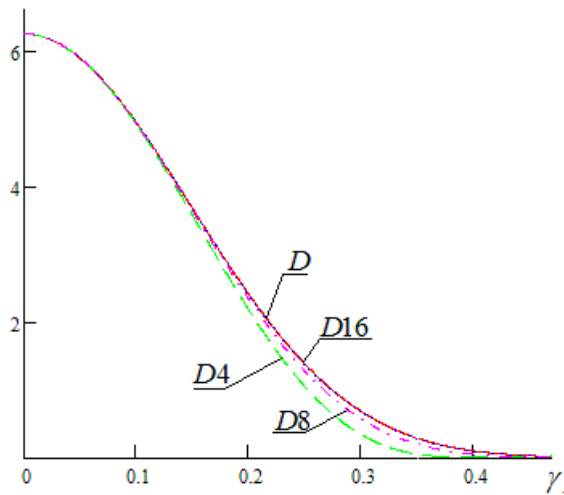


Fig. 4 - Graph of changing  $D$ ,  $D4$ ,  $D8$ ,  $D16$

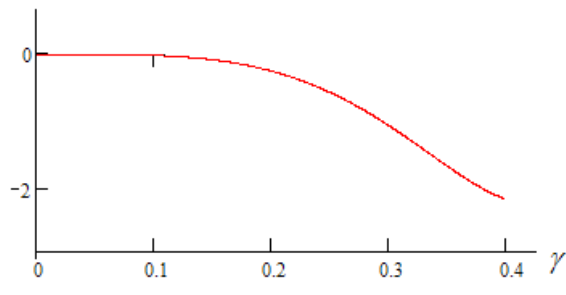


Fig. 5- Graph of changing relative error approximation function  $D$  by  $D16$

According to the Vard model, the color intensity is determined by the following formula

$$I_w = \frac{k_d}{\pi} + k_s \cdot \frac{1}{\sqrt{\vec{V} \cdot \vec{N} + \vec{L} \cdot \vec{H}}} \cdot \frac{e^{-\frac{tg^2(\gamma)}{m^2}}}{4 \cdot \pi \cdot \alpha^2}$$

where  $\alpha$  - correction coefficient that depends on the curvature of the surface,

The difference between the Vard model and the Cook-Torrance model is the absence of the Fresnel factor [] and the self-shadowing factor. It is believed that Vard in his model has reached the most accurate fit of this model to the experimental data.

Replace  $e^{-\frac{tg^2(\gamma)}{m^2}}$  on  $\cos^{\frac{2}{g}}(\gamma)$ . Using these in the second chapter we can rewrite

dependence  $\cos^n \gamma \approx \left( \frac{n}{g} (\cos \gamma - 1) + 1 \right)^g$  as

$$\begin{aligned} I_w &\approx \frac{k_d}{\pi} + k_s \cdot \frac{1}{\sqrt{\vec{V} \cdot \vec{N} + \vec{L} \cdot \vec{H}}} \cdot \frac{\cos^{\frac{2}{g}}(\gamma)}{4 \cdot \pi \cdot \alpha^2} = \frac{k_d}{\pi} + k_s \cdot \frac{1}{\sqrt{\vec{V} \cdot \vec{N} + \vec{L} \cdot \vec{H}}} \cdot \frac{\cos^{\frac{2}{g}}(\gamma)}{4 \cdot \pi \cdot \alpha^2} = \\ &= \frac{k_d}{\pi} + k_s \cdot \frac{1}{\sqrt{\vec{V} \cdot \vec{N} + \vec{L} \cdot \vec{H}}} \cdot \frac{\left( \frac{2}{g \cdot m^2} (\cos \gamma - 1) + 1 \right)^g}{4 \cdot \pi \cdot \alpha^2}. \end{aligned}$$

The analysis showed that a sufficient approximation accuracy achieved with  $g = 16$ .

In this case

$$I_w = \frac{k_d}{\pi} + k_s \cdot \frac{1}{\sqrt{\vec{V} \cdot \vec{N} + \vec{L} \cdot \vec{H}}} \cdot \frac{\left( \frac{1}{8 \cdot \alpha^2} (\cos \gamma - 1) + 1 \right)^{16}}{4 \cdot \pi \cdot \alpha^2}.$$

The relative error of approximation  $e^{-\frac{tg^2(\gamma)}{m^2}}$  does not exceed 1.3%.

The proposed expressions have significantly less computational complexity than the original expressions by using only one function, and to a lesser extent. Figure 6 shows examples of image formation using the developed Cook-Torrence and Vard models.

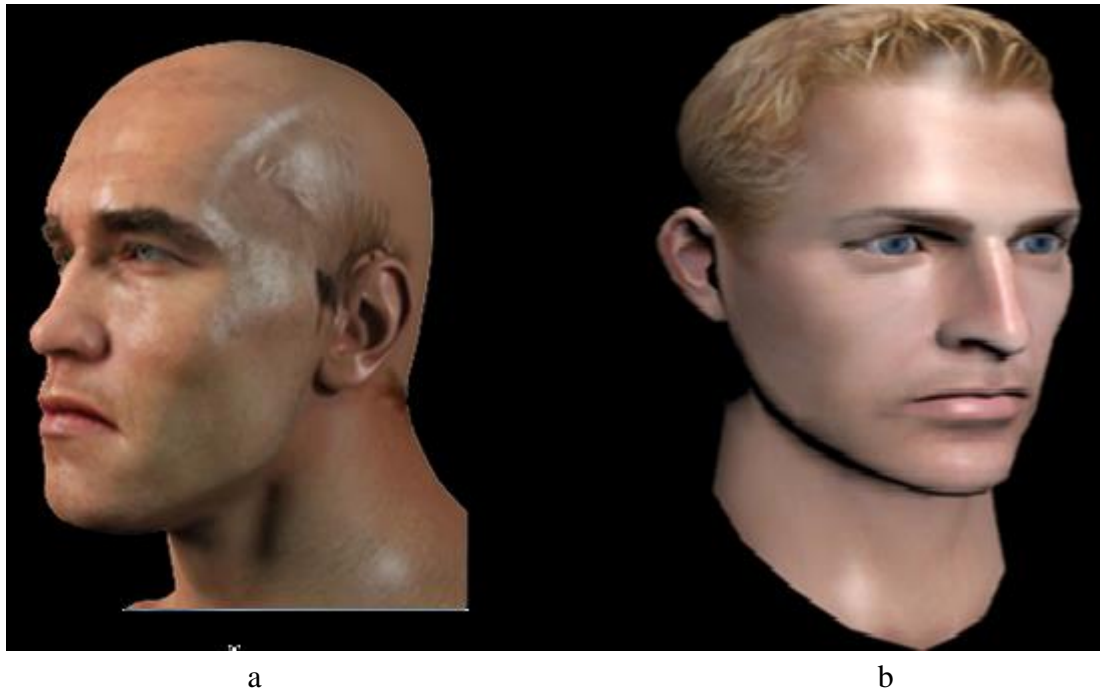


Fig. 6 examples of face images rendering using the developed modified models a – Cook-Torrence model, b – Vard model.

#### **Research results.**

A modification of the Cook-Torrence model is proposed by using a new formula to determine the parameter used to calculate the rms slope of the microgranules. The analysis

showed that when using the parameter  $D = \frac{1}{4 \cdot m^2} \cdot \left[ \left( \frac{1}{8 \cdot m^2} - \frac{1}{4} \right) \cdot (\cos(\gamma) - 1) + 1 \right]^{16}$

against  $D = \frac{e^{-\frac{tg^2(\gamma)}{m^2}}}{4 \cdot m^2 (\vec{H} \cdot \vec{N})^4}$  allowed to increase the productivity of its calculation by 4.34

times. For the Varda model, productivity gains are more than twice.

#### **IV. DEVELOPMENT OF AN ADAPTIVE METHOD OF DETERMINING THE DIFFUSE AND SPECULAR COMPONENTS FOR RENDERING [2]**

Today surgeries during plastic surgery can be estimated by constructing 3D models. This makes it possible to reduce differences and dissatisfaction on the part of patients and reduce the risk of such transactions to the lowest level .. have a unique opportunity ahead of time to see



how a person will look after the work of plastic surgeons [9, 11]. In forming the 3D image rights should be as accurately reproduce real face. It is important to convey realistic colors. Therefore, the formation of diffuse and specular color components put forward higher requirements. Formation diffuse color component images of areas face a complex computational problem, since each pixel must calculate surface color intensity, which is necessary to define the inner product unit vectors to the light source and the normal to the surface. Determination unit vectors involves normalizing output vector that require labor-intensive operations perform multiplication, division and square root of. Therefore, the actual problem is facilitation of procedures diffuse color component without substantial loss of realism of the final image. In [7] for finding the diffuse color component offered rasterization line break at intervals, except for the last, each of which use linear interpolation [6]. The proposed method is highly effective only for surfaces with small curvature. Failing to provide acceptable accuracy must break line rasterization on a large number of intervals, which significantly reduces the efficiency calculations. In addition, the appearance of artifacts within at intervals not considered as differentiation curve for color intensity.

The use of quadratic interpolation [4] to find intensity of color components makes it possible to increase the size ranges, but use as a parabola curve color intensity can distort the real curve and consequently lead to low precision calculations.

Intensity of use for the current color component range line rasterization a polynomial of the third degree,

$$I_{i,t} = A_i \cdot t^3 + B_i \cdot t^2 + C_i \cdot t + D_i$$

where  $t$  - parametric variable  $A_i, B_i, C_i, D_i$  - unknown to be found by determining the color intensity interval at four points, which is broken line rasterization. Find the unknown  $A_i, B_i, C_i, D_i, I_{i,t}$  - the intensity of the diffuse or specular color component.

Obviously, when  $t=0$   $I_{i,l} = D_i$ . At the end point of the interval  $t=1$ . Ago  $I_{i,p} = A_i + B_i + C_i + D_i$ . At the midpoint of the interval  $t=1/2$ , ago  $I_{i,c} = \frac{A_i}{8} + \frac{B_i}{4} + \frac{C_i}{2} + D_i$ . At the point  $t=1/4$   $I_{i,c} = \frac{A_i}{64} + \frac{B_i}{16} + \frac{C_i}{4} + D_i$ .

Thus, to find unknown  $A_i, B_i, C_i, D_i$  you can create a system of equations

$$\begin{cases} I_{i,l} = D_i, \\ I_{i,p} = A_i + B_i + C_i + D_i, \\ I_{i,c} = \frac{A_i}{8} + \frac{B_i}{4} + \frac{C_i}{2} + D_i, \\ I_{i,c2} = \frac{A_i}{64} + \frac{B_i}{16} + \frac{C_i}{4} + D_i. \end{cases}$$

Solution reduced system of equations gives the following formula to determine the unknown coefficients:

$$A = \frac{8(I_2 + 8 \cdot I_4)}{3} - 8(I_1 + 2 \cdot I_3) \quad B = 2(7 \cdot I_1 - I_2 + 10 \cdot I_3 - 16 \cdot I_4)$$

$$A = \frac{I_2 + 32 \cdot I_4}{3} - 7 \cdot I_1 - 4 \cdot I_3 \quad D = I_1,$$

We use to compile a system of equations such point interval:

$t=0, t=\frac{1}{2}, t=\frac{3}{4}, t=1$ . We obtain a system of equations

$$\begin{cases} I_{i,l} = D_i, \\ I_{i,p} = A_i + B_i + C_i + D_i, \\ I_{i,c} = \frac{A_i}{8} + \frac{B_i}{4} + \frac{C_i}{2} + D_i, \\ I_{i,c2} = \frac{A_i \cdot 27}{64} + \frac{B_i \cdot 9}{16} + \frac{C_i \cdot 3}{4} + D_i. \end{cases}$$

The solution is a system

$$A = 8 \cdot (I_2 + 2 \cdot I_3) - \frac{8 \cdot (8 \cdot I_4 + I_1)}{3}, \quad B = 2 \cdot (3 \cdot I_1 - 5 \cdot I_2 - 14 \cdot I_3 + 16 \cdot I_4),$$

$$D = I_1, \quad C = 3 \cdot (I_2 + 4 \cdot I_3) - \frac{13 \cdot I_1 + 32 \cdot I_4}{3}.$$

In these formulas are many factors to power of two, which simplifies hardware implementation, as in this case, micro-multiplication can be replaced by micro assembly shift. In addition, many factors can set the amount of values that are equal degree two, for example,  $10 \cdot I = 8 \cdot I + 2 \cdot I$ . It also replace micro multiplication by addition and shift. Given this is the first time the most appropriate.

Division 3 can also be implemented using shift and add. For example,

$$\frac{1}{3} \approx \frac{1}{2} - \frac{1}{8} - \frac{1}{32} - \frac{1}{128}.$$

In this case, the relative proportion of error of no more than 0.79%.

Fig. 7 shows a functional block diagram of the portion  $I / 3$ .

Fig. 8 shows an example hardware implementation factor  $B_i$  without operations of multiplication and division by adding operands shifted towards senior level.

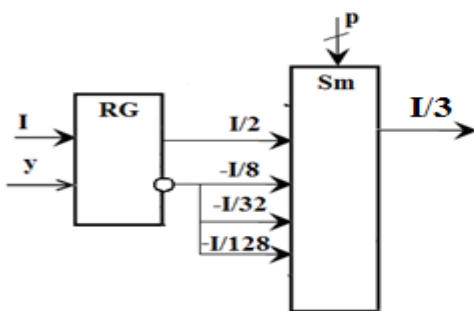


Fig. 7 Functional block diagram the portion  $I / 3$

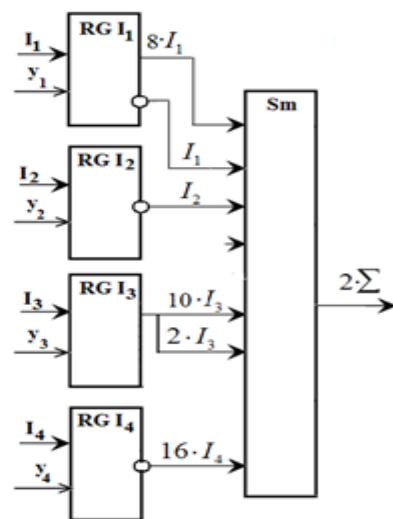


Fig. 8 A functional block diagram of of armatures determining factor

Similar is the construction unit to determine other factors.

Fig. 9 shows a functional block diagram for determining the color intensity using a polynomial of the third degree. For this uses the relationship

$$I_{i,t} = A_i \cdot t^3 + B_i \cdot t^2 + C_i t + D_i = t \cdot (t \cdot (A_i \cdot t + B_i) + C_i) + D_i.$$

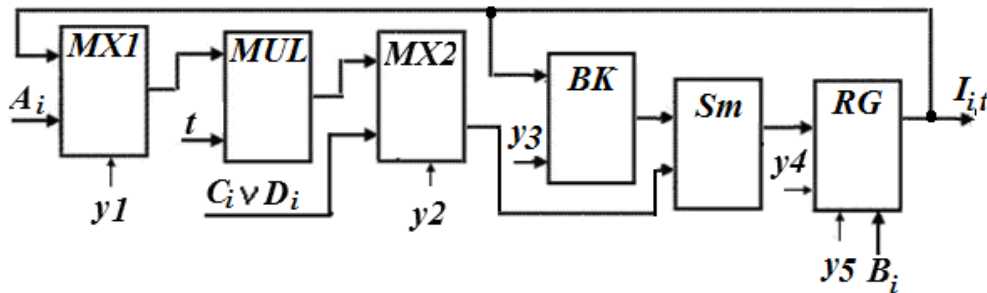


Fig. 9 A functional block for determining the color intensity using a polynomial of the third degree

In registry *RG* entered value  $B_i$ , and input *MX1* submitted values  $A$  That the block *MUL* multiplied by the value  $t$ . Therefore, the output of the adder *Sm* determined value  $(A_i \cdot t + B_i)$  Which is stored in the register *RG*. This iteration of block valves *BK* operates in transmit mode operand.

Block key switch reset mode operand. Value  $(A_i \cdot t + B_i)$  multiplied by  $t$  and recorded in the register *RG*. The output of the adder *Sm* formed importance  $(A_i \cdot t + B_i) \cdot t$ .

The input multiplexer *MX2* submit value  $C_i$  Because the output of the adder *Sm* formed importance  $(t \cdot (A_i \cdot t + B_i) + C_i)$  Be entered in the register *RG*. To block this key switch the transmission mode operand.

Subsequently, the resulting value is multiplied by  $t$ . In this case, block key resets value stored in the register *RG*. Block key switch in transmission mode operand. Subsequently, the input multiplexer *MX2* submit value  $D_i$  That is added to the operand  $t \cdot (t \cdot (A_i \cdot t + B_i) + C_i)$  That gives a output register *RG* value  $I_{i,t}$ .

Fig. 10 shows the splitting image of a human face on specific areas. The analysis showed that for lots 2, 4, 7 expedients to use for determining the diffuse and specular components approximating polynomial of the second degree, but for others - the third degree.

The Fig. 11 shows an example of forming a three-dimensional image of the face using the adaptive method of painting.



Fig. 10 Distinguish of face for specific areas

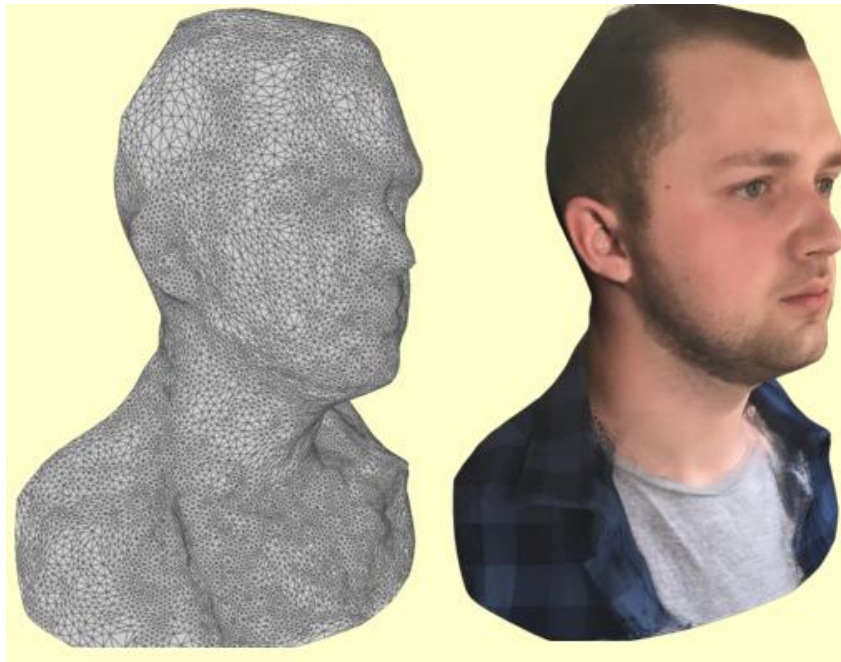


Fig. 11 Example of forming a three-dimensional image of the face using the adaptive method of painting

**Research results.**

Analysis of the complexity of imaging the human face under the proposed method showed that compared with Phong achieved by increasing productivity up to 3 times by reducing the number of long-term operations and multiplication and division of the square root. Adaptive use of polynomials of second and third degrees possible to achieve normalized mean square error (NMSE) not more than 0.0001, which means that the image formed face of visually indistinguishable relative image formed by the method Phong.

The proposed method and models can be used in highly realistic computer graphics systems.

## CONCLUSION

The paper proposes a new method and models for high-performance face rendering. Scientific novelty of the obtained results.

1. The method of painting is developed, the peculiarity of which is the adaptive use for determining the intensities of color in different parts of the surface of the polynomials of the second and third degrees, which allowed to increase the productivity of forming a three-dimensional image, and, as a consequence, to provide a dynamic mode of display.
2. New modifications of the Cook-Torrence and Vard models are proposed, which differ from the known uses when calculating only one function and smaller degrees of polynomials, which makes it possible to improve the performance of three-dimensional image formation taking into account the offset properties of surfaces.
3. Expressions for approximating polynomials to determine the speculative and diffuse color components are proposed, which made it possible to improve the productivity of face imaging.
4. Hardware has been developed to determine the color intensities, which makes it possible to implement a high-speed specialized device.
5. The areas of the face are selected for the adaptive use of approximating polynomials, which makes it possible to increase the realistic formation of graphic images.

The practical significance of the obtained results is that, on the basis of theoretical studies and scientific results obtained, software and hardware for the formation of three-dimensional images have been developed.

## REFERENCES

- [1] Вяткин С. И., Романюк А. Н., Трояновская Т. И., Нечипорук Н. Л. Синтез двунаправленных текстурных функций для функционально заданных поверхностей / С. И. Вяткин, А. Н. Романюк, Т. И. Трояновская, Н. Л. Нечипорук // Наукові праці Донецького національного технічного університету. Серія : Інформатика, кібернетика та обчислювальна техніка. - 2018. - № 2. - С. 46-52. - Режим доступу: <http://nbuv.gov.ua/UJRN/>
- [2] Павлов С. В., Романюк С. О., Нечипорук М. Л. Адаптивне визначення дифузної та спекулярної складових кольору для рендерингу зображень обличчя при плануванні пластичних операцій / С. В. Павлов, С. О. Романюк, М. Л. Нечипорук // Scientific Journal «ScienceRise». № 8: 24-28., 2018 р.
- [3] Романюк О. Н. Аналіз методів зафарбовування поверхонь тривимірних об'єктів / О. Н. Романюк, В. О. Отришко, М. Л. Нечипорук // Збірник доповідей міжнародної науково-технічної конференції «Комп'ютерна графіка та розпізнавання зображень». – 2019. – С. 140-144.
- [4] Романюк О. Н. Використання квадратичної інтерполяції для зафарбовування тривимірних графічних об'єктів // Реєстрація, зберігання і обробка даних. 2006. Т. 8, № 4. С. 31–37.
- [5] Романюк О. Н. Ефективна модель для відтворення спекулярної складової кольору: зб. наук. пр. // Проблеми інформатизації та управління. 2007. № 2 (20). С. 115–120.
- [6] Романюк О. Н., Нечипорук М. Л., Лисенко Є. С. Модифікований метод лінійної інтерполяції / О. Н. Романюк, М. Л. Нечипорук, Є. С. Лисенко // Електронні інформаційні ресурси : створення, використання, до-ступ : збірник матеріалів Міжнародної науково-практичної інтернет-конференції, м. Вінниця, листопад 2017 р. – С. 236-240.
- [7] Романюк О. Н., Чорний А. В. Високопродуктивні методи та засоби зафарбовування тривимірних графічних об'єктів: монографія / О.Н. Романюк, А. В. Чорний. Вінниця: УНІВЕСУМ-Вінниця, 2006. 190 с.
- [8] Романюк О.Н., Нечипорук М.Л. Використання морфінгу зображень для медичних застосувань/ О.Н. Романюк, М.Л.Нечипорук // Матеріали ІІ Міжнародної науково-практичної конференції ІТ-професіоналів та аналітиків комп'ютерних систем “ProfIT Conference”, м.Харків, 2019. - С. 23-24.
- [9] Романюк О.Н., Павлов С.В., Нечипорук М.Л. Комп'ютерна програма «Програма для краніометричних вимірювань голови людини» / О.Н. Романюк, С.В. Павлов, М.Л. Нечипорук / Свідectво про реєстрацію авторського права на твір № 92336. Державний департамент інтелектуальної власності України. 23.09.2019

- [10] Романюк О.Н., Павлов С.В., Тимчик С.В., Нечипорук М.Л. Комп'ютерна програма «Програма для аналізу відповідності вікових змін розвитку людини встановленим нормам з використанням морфінгу зображень О.Н. Романюк, С.В., Павлов С.В. Тимчик, М.Л. Нечипорук / Свідectво про реєстрацію авторського права на твір № 92335. Державний департамент інтелектуальної власності України. 23.09.2019
- [11] Романюк С. О., Нечипорук М. Л. Фотограмметричні комп'ютерні засоби отримання 3D-моделей зображень обличчя людини / С. О. Романюк, М. Л. Нечипорук // XI міжнародна науково-практична конференція "Інформаційні технології і автоматизація – 2018", Одеса, 4 – 5 жовтня 2018 р. – 2018. – Ч. II. – С. 10-12.
- [12] Романюк С.О., Нечипорук М.Л. Комп'ютерна програма для визначення інтенсивності відбитого світла з використанням моделі Кука-Торенса / С.О Романюк., М.Л. Нечипорук / Свідectво про реєстрацію авторського права на твір № 84717.. Державний департамент інтелектуальної власності України. 22.01.2019.
- [13] Херн Д., Бейкер М. Компьютерная графика и стандарт OpenGL. Москва: Издательский дом "Вильямс", 2005. 1168 с.
- [14] Цисарж В. В. Математические методы компьютерной графики. Киев: Факт, 2004. 464 с.
- [15] Vyatkin S. I., Romaniuk A. N., Nechiporuk M. L., Roptanov V. I. The method of splatting the filter-based weighted average / S. I. Vyatkin, A. N. Romaniuk, M. L. Nechiporuk, V. I. Roptanov // International scientific publication "World scientific and technical trends' 2018" : conference proceedings, 25-26 December 2018. – 2018. – P. 14-15.
- [16] Vyatkin S. I., Romanyuk A.N., Romanyuk O., Vasilyevich S.A., Nechiporuk M.L. Shadow Generation Method for Volume-Oriented Visualization of Functionally Defined Objects / S. Vyatkin, A.N. Romanyuk, O. Romanyuk, S. A. Vasilyevich and M.L. Nechiporuk // 2019 9th International Conference on Advanced Computer Information Technologies (ACIT), Ceske Budejovice, Czech Republic, 2019, pp. 470-474. doi: 10.1109/ACITT.2019.878010. (SCOPUS)
- [17] Vyatkin S.I, Romanyuk A.N., Nechiporuk M.L., Romanyuk O., Troianovska T. Visualization of volumetric data and functionally defined surfaces using graphics processing units / S.I. Vyatkin, A.N. Romanyuk, M.L. Nechiporuk, O. Romanyuk, T. Troianovska P. 216-228. ISBN 978-3-953794-29-8. (SCOPUS)
- [18] Vyatkin S.I., Romanyuk A.N., Troianovska T., Tsikhanovska O., Nechiporuk M.L., Lysenko I. Convolution Surfaces using Volume Bounding / S.I. Vyatkin, A.N. Romanyuk, T. Troianovska, O. Tsikhanovska, M. Nechiporuk, I. Lysenko // 2019 9th International Conference on Advanced Computer Information Technologies (ACIT), Ceske Budejovice, Czech Republic, 2019, pp. 461-465. doi: 10.1109/ACITT.2019.8779894. (SCOPUS)